LC-TH-2000-032
DESY 00-002
UWThPh-2000-3
WUE-ITP-2000-004
HEPHY-PUB 726/2000
hep-ph/0002253

Exploiting Spin Correlations in Neutralino Production and Decay with Polarized e^- and e^+ Beams [1]

G. Moortgat–Pick[a2], A. Bartl[b3], H. Fraas[c4], W. Majerotto[d5]

[a] *DESY, Deutsches Elektronen–Synchrotron, D–22603 Germany*
[b] *Institut für Theoretische Physik, Universität Wien, A–1090 Wien, Austria*
[c] *Institut für Theoretische Physik, Universität Würzburg, D–97074 Würzburg, Germany*
[d] *Institut für Hochenergiephysik der Österreichischen Akademie der Wissenschaften, A–1050 Wien, Austria*

Abstract

We study the production process $e^+e^- \to \tilde{\chi}^0_1\tilde{\chi}^0_2$ and the subsequent decay $\tilde{\chi}^0_2 \to \tilde{\chi}^0_1\ell^+\ell^-$ with polarized e^+ and e^- beams, including the spin correlations between production and decay. We work out the advantages of polarizing both beams. We study in detail the angular distribution and the forward–backward asymmetry of the decay lepton ℓ^- as well as the opening angle distribution between the decay leptons. We investigate the dependence on the masses of $\tilde{e}_L$ and $\tilde{e}_R$ and on the mixing character of the neutralinos. In particular we study the dependence on the gaugino mass parameter M_1.

[1]Contribution to the Proceedings of the 2nd Joint ECFA/DESY study on Physics and Detectors for a Linear Electron-Positron Collider

[2]e-mail: gudrid@mail.desy.de
[3]e-mail: bartl@ap.univie.ac.at
[4]e-mail: fraas@physik.uni-wuerzburg.de
[5]e-mail: majer@qhepu3.oeaw.ac.at.

1 Introduction

The search for supersymmetric (SUSY) particles and the determination of their properties will be one of the main goals of a future e^+e^- linear collider. Particularly interesting will be the experimental study of the neutralinos, which are the quantum mechanical mixtures of the neutral gauginos and higgsinos, the SUSY partners of the neutral gauge and Higgs bosons. In the Minimal Supersymmetric Standard Model (MSSM) there are four neutralinos $\tilde{\chi}^0_i$, $i = 1, \ldots, 4$. In extensions of the MSSM there may be more than four neutralinos. Usually the lightest neutralino $\tilde{\chi}^0_1$ is the lightest SUSY particle LSP. Therefore, the production of the lightest and the second lightest neutralino can presumably be studied at an e^+e^- linear collider with a CMS energy $\sqrt{s} = 500$ GeV. The aim will be to precisely determine the SUSY parameters of the neutralino system. By a detailed study of the neutralino system one can also examine the question whether the MSSM or another SUSY model is realized in nature. Models with an extended neutralino sector have been discussed in [1]. Recently a method for determining the SUSY parameter M_2, μ and $\tan\beta$ by measuring suitable observables in chargino production $e^+e^- \to \tilde{\chi}^+_i \tilde{\chi}^-_j$ $(i, j = 1, 2)$ has been proposed in [2]. The process $e^+e^- \to \tilde{\chi}^+_i \tilde{\chi}^-_j$, $\tilde{\chi}^+_i \to \tilde{\chi}^0_k \ell^+ \nu$ including the full spin correlation has been studied in [3].

In previous papers (see [4, 5] and references therein) the cross sections of $e^+e^- \to \tilde{\chi}^0_i \tilde{\chi}^0_j$, $i, j = 1 \ldots 4$, and the branching ratios and energy distributions of neutralino decays were studied, which do not depend on spin correlations. In the calculation of the decay angular distributions, however, one has to take into account the spin correlations between production and decay of the neutralinos. In [6] we have studied the process $e^+e^- \to \tilde{\chi}^0_i \tilde{\chi}^0_j$ with unpolarized beams and the subsequent leptonic decays $\tilde{\chi}^0_i \to \tilde{\chi}^0_k \ell^+ \ell^-$ including the complete spin correlations. In [7] we have given the complete analytical formulae for longitudinally polarized beams, including the spin correlations between production and decay. The formulae have been given in the laboratory system in terms of the basic kinematic variables.

In the present paper we extend our analysis in [7] and study neutralino production in the case that both beams are polarized. We show that by a suitable choice of the e^+ beam polarization not only higher cross sections but also additional information can be gained. We give numerical predictions for the process $e^+e^- \to \tilde{\chi}^0_1 \tilde{\chi}^0_2$ with $\tilde{\chi}^0_2 \to \tilde{\chi}^0_1 e^+ e^-$ including the full spin correlations between production and decay. The Feynman diagrams are shown in Fig. 1. The framework of our studies is the MSSM. We first assume the GUT relation $M_1/M_2 = \frac{5}{3}\tan^2\Theta_W$ for the gaugino mass parameters (note that in Refs. [4, 6, 7] we used the notation M' and M for M_1 and M_2). We consider two gaugino–like and one higgsino–like scenario and study the dependence of the cross section, the forward–backward asymmetry of the decay electron, and the opening angle distribution of the decay lepton pair e^+ and e^- on the beam polarizations and on the masses of the exchanged $\tilde{e}_L$ and $\tilde{e}_R$. Then we relax the GUT relation between M_1 and M_2 and study the M_1 dependence of $\sigma(e^+e^- \to \tilde{\chi}^0_1\tilde{\chi}^0_2) \times BR(\tilde{\chi}^0_2 \to \tilde{\chi}^0_1 e^+e^-)$ and the forward-backward asymmetry of the decay electron for various beam polarizations and slepton masses. We also discuss which observables are suitable for the determination of the neutralino parameters and selectron masses.

2 Spin correlations between production and decay

Both the helicity amplitudes $T_P^{\lambda_i\lambda_j}$ for the production process $e^-(p_1)e^+(p_2) \to \tilde{\chi}^0_i(p_3,\lambda_i)\tilde{\chi}^0_j(p_4,\lambda_j)$ and the helicity amplitudes T_{D,λ_i} and T_{D,λ_j} for the decay processes $\tilde{\chi}^0_i(p_3,\lambda_i) \to \tilde{\chi}^0_k(p_5)\ell^+(p_6)\ell^-(p_7)$ and $\tilde{\chi}^0_j(p_4,\lambda_j) \to \tilde{\chi}^0_l(p_8)\ell^+(p_9)\ell^-(p_{10})$, respectively, receive contributions from Z^0 exchange in the direct channel and from $\tilde{e}_{L,R}$ exchange in the crossed channels.

The amplitude squared of the combined process of production and decay is (summed over helicities):

$$|T|^2 = |\Delta(\tilde{\chi}^0_i)|^2|\Delta(\tilde{\chi}^0_j)|^2\rho_P^{\lambda_i\lambda_j\lambda'_i\lambda'_j}\rho_{D,\lambda'_i\lambda_i}\rho_{D,\lambda'_j\lambda_j}. \tag{1}$$

It is composed of the (unnormalized) spin density production matrix

$$\rho_P^{\lambda_i\lambda_j\lambda'_i\lambda'_j} = T_P^{\lambda_i\lambda_j}T_P^{\lambda'_i\lambda'_j *}, \tag{2}$$

the decay matrices

$$\rho_{D,\lambda'_i\lambda_i} = T_{D,\lambda_i}T^*_{D,\lambda'_i} \quad \text{and} \quad \rho_{D,\lambda'_j\lambda_j} = T_{D,\lambda_j}T^*_{D,\lambda'_j}, \tag{3}$$

and the propagator

$$\Delta(\tilde{\chi}^0_k) = 1/[p_k^2 - m_k^2 + im_k\Gamma_k]. \tag{4}$$

Here p_k^2, λ_k, m_k and Γ_k denote the four–momentum squared, helicity, mass and total width of $\tilde{\chi}^0_k$. For this propagator we use the narrow–width approximation.

Introducing a suitable set of polarization vectors for each of the neutralinos the density matrices can be expanded in terms of Pauli matrices σ^a:

$$\begin{aligned}
\rho_P^{\lambda_i\lambda_j\lambda'_i\lambda'_j} &= (\delta_{\lambda_i\lambda'_i}\delta_{\lambda_j\lambda'_j}P(\tilde\chi^0_i\tilde\chi^0_j) + \delta_{\lambda_j\lambda'_j}\sum_{a=1}^{3}\sigma^a_{\lambda_i\lambda'_i}\Sigma^a_P(\tilde\chi^0_i) \\
&\quad +\delta_{\lambda_i\lambda'_i}\sum_{b=1}^{3}\sigma^b_{\lambda_j\lambda'_j}\Sigma^b_P(\tilde\chi^0_j) + \sum_{a,b=1}^{3}\sigma^a_{\lambda_i\lambda'_i}\sigma^b_{\lambda_j\lambda'_j}\Sigma^{ab}_P(\tilde\chi^0_i\tilde\chi^0_j)), \qquad (5)\\
\rho_{D,\lambda'_i\lambda_i} &= (\delta_{\lambda'_i\lambda_i}D(\tilde\chi^0_i) + \sum_{a=1}^{3}\sigma^a_{\lambda'_i\lambda_i}\Sigma^a_D(\tilde\chi^0_i)), \qquad (6)\\
\rho_{D,\lambda'_j\lambda_j} &= (\delta_{\lambda'_j\lambda_j}D(\tilde\chi^0_j) + \sum_{b=1}^{3}\sigma^b_{\lambda'_j\lambda_j}\Sigma^b_D(\tilde\chi^0_j)). \qquad (7)
\end{aligned}$$

We choose the polarization vectors such that $\Sigma^1_P(\tilde\chi^0_{i,j})$ describes the transverse polarization in the production plane, $\Sigma^2_P(\tilde\chi^0_{i,j})$ denotes the polarization perpendicular to the production plane and $\Sigma^3_P(\tilde\chi^0_{i,j})$ describes the longitudinal polarization of the respective neutralino. $\Sigma^{ab}_P(\tilde\chi^0_i\tilde\chi^0_j)$ is due to correlations between the polarizations of both neutralinos. The complete analytical expressions for the production density matrix and for the decay matrices are given in [7].

If CP is conserved the neutralino couplings can be chosen real. It can be seen in [7] that in this case, due to the Majorana character of the neutralinos, the quantities P, Σ^1_P, Σ^{11}_P, Σ^{22}_P, Σ^{33}_P, Σ^{23}_P are symmetric under the exchange $\cos\Theta \leftrightarrow -\cos\Theta$, where Θ is the production angle of p_4. The quantities Σ^2_P, Σ^3_P, Σ^{12}_P, Σ^{13}_P are forward–backward antisymmetric.

The amplitude squared $|T|^2$ (1) of the combined process of production and decay can be rewritten as:

$$\begin{aligned}
|T|^2 = 4|\Delta(\tilde\chi^0_i)|^2|\Delta(\tilde\chi^0_j)|^2\Big(&P(\tilde\chi^0_i\tilde\chi^0_j)D(\tilde\chi^0_i)D(\tilde\chi^0_j) + \sum_{a=1}^{3}\Sigma^a_P(\tilde\chi^0_i)\Sigma^a_D(\tilde\chi^0_i)D(\tilde\chi^0_j)\\
&+\sum_{b=1}^{3}\Sigma^b_P(\tilde\chi^0_j)\Sigma^b_D(\tilde\chi^0_j)D(\tilde\chi^0_i) + \sum_{a,b=1}^{3}\Sigma^{ab}_P(\tilde\chi^0_i\tilde\chi^0_j)\Sigma^a_D(\tilde\chi^0_i)\Sigma^b_D(\tilde\chi^0_j)\Big). \qquad (8)
\end{aligned}$$

The differential cross section is then given by

$$d\sigma_e = \frac{1}{2s}|T|^2(2\pi)^4\delta^4(p_1+p_2-\sum_i p_i)d\mathrm{lips}(p_3\ldots p_{10}), \qquad (9)$$

where $d\mathrm{lips}(p_3,\ldots,p_{10})$ is the Lorentz invariant phase space element.

If one neglects all spin correlations between production and decay only the first term in (8) contributes. The second and third term in (8) describe the spin correlations between the production and the decay process and the last term is due to spin–spin correlations between both decaying neutralinos.

3 Numerical analysis and discussion

In the MSSM [8] the masses and couplings of neutralinos are determined by the parameters M_1, M_2, μ, $\tan\beta$, which can be chosen real if CP violation is neglected. Moreover, one usually makes use of the GUT relation

$$M_1 = \frac{5}{3} M_2 \tan^2 \Theta_W. \tag{10}$$

The neutralino mass mixing matrix in the convention used here can be found in [4].

The total cross section of $e^+e^- \to \tilde{\chi}^0_i \tilde{\chi}^0_j$ and the decay rate $\tilde{\chi}^0_i \to \tilde{\chi}^0_k e^+ e^-$ further depend on the masses of $\tilde{e}_L$ and $\tilde{e}_R$. In the following numerical analysis we study neutralino production and decay in three scenarios, which we denote by A1, A2, and B. The corresponding parameters are given in Table 1.

Scenario A1 corresponds to that in [9]. In this scenario $\tilde{\chi}^0_1$ is $\tilde{B}$–like and $\tilde{\chi}^0_2$ is $\tilde{W}^3$–like. The selectron masses are $m_{\tilde{e}_L} = 176$ GeV, $m_{\tilde{e}_R} = 132$ GeV. Scenario A2 differs from A1 only by the higher mass $m_{\tilde{e}_L} = 500$ GeV. In scenario B the same masses as in scenario A1 are taken for $\tilde{\chi}^0_1$, $\tilde{\chi}^0_2$, $\tilde{e}_L$, $\tilde{e}_R$. $\tilde{\chi}^0_1$ and $\tilde{\chi}^0_2$ are, however, higgsino–like due to the choice $\mu < M_2$.

3.1 Effects of beam polarizations on the total cross section

The cross section $\sigma(e^+e^- \to \tilde{\chi}^0_1 \tilde{\chi}^0_2)$ is shown in Figs. 2a–c as a function of the longitudinal beam polarizations P^3_- for electrons and P^3_+ for positrons, for scenario A1, A2 and B, respectively, (with $P^3_\pm = \{-1, 0, 1\}$ for {left–, un–, right–}polarized). In scenario B the $Z\tilde{\chi}^0_1\tilde{\chi}^0_2$ coupling is large because $\tilde{\chi}^0_1$ and $\tilde{\chi}^0_2$ are higgsino–like. Therefore the cross section is larger than in scenarios A1 and A2. The cross sections are shown at $\sqrt{s} = (m_{\tilde{\chi}^0_1} + m_{\tilde{\chi}^0_2}) + 30$ GeV.

In Figs. 2a–c the white area is accessible by an electron polarization $|P^3_-| \leq 85\%$ and a positron polarization $|P^3_+| \leq 60\%$. The cross section can be enhanced by a factor 2–3 by polarizing both beams. Theoretically, for pure gaugino–like neutralinos and $m_{\tilde{e}_L} \gg m_{\tilde{e}_R}$ ($m_{\tilde{e}_L} \ll m_{\tilde{e}_R}$) and $P^3_- = +1$, $P^3_+ = -1$ ($P^3_- = -1$, $P^3_+ = +1$), the cross section could be enlarged by a factor 4. For pure higgsino–like neutralinos and $P^3_- = +1$, $P^3_+ = -1$ ($P^3_- = -1$, $P^3_+ = +1$) this factor would be 1.7 (2.3) [10].

One clearly recognizes the dependence of the cross section on the selectron masses $m_{\tilde{e}_L}$ and $m_{\tilde{e}_R}$ as well as on the mixing character of $\tilde{\chi}^0_1$ and $\tilde{\chi}^0_2$. In scenario A2 with $m_{\tilde{e}_L} \gg m_{\tilde{e}_R}$ and gaugino–like $\tilde{\chi}^0_{1,2}$, one expects the largest cross section for $P^3_- = +1$ and $P^3_+ = -1$, see Fig. 2b. In scenario B the cross section is governed by Z^0 exchange and is therefore rather symmetric for $P^3_- = \pm \leftrightarrow P^3_+ = \mp$. The beam polarizations are a useful tool for getting more information about $m_{\tilde{e}_L}$ and $m_{\tilde{e}_R}$.

If the polarizations of both beams are varied, the relative size of the cross sections strongly depends on the mixing character of both neutralinos $\tilde{\chi}^0_{1,2}$ and on the selectron masses [10]. If $\tilde{\chi}^0_1$ and $\tilde{\chi}^0_2$ are pure higgsinos, one obtains for $|P^3_-| = 85\%$ and $|P^3_+| = 60\%$ the sequence

$$\sigma_e^{-+} > \sigma_e^{+-} > \sigma_e^{-0} > \sigma_e^{00} > \sigma_e^{+0} > \sigma_e^{--} > \sigma_e^{++}. \tag{11}$$

Here σ_e is given by

$$\sigma_e = \sigma(e^- e^+ \to \tilde{\chi}^0_1 \tilde{\chi}^0_2) \times BR(\tilde{\chi}^0_2 \to \tilde{\chi}^0_1 \ell^+ \ell^-) \tag{12}$$

and $(-+)$ etc. denotes the sign of the electron polarization P^3_- and of the positron polarization P^3_+, respectively.

If $\tilde{\chi}^0_1$ and $\tilde{\chi}^0_2$ are pure gauginos the order of the cross sections depends on the relative magnitude of the selectron masses $m_{\tilde{e}_L}$ and $m_{\tilde{e}_R}$. For $m_{\tilde{e}_L} \gg m_{\tilde{e}_R}$ only right selectron exchange contributes, and one obtains

$$\sigma_e^{+-} > \sigma_e^{+0} > \sigma_e^{00} > \sigma_e^{++} > \sigma_e^{--} > \sigma_e^{-0} > \sigma_e^{-+}, \tag{13}$$

whereas for $m_{\tilde{e}_R} \gg m_{\tilde{e}_L}$, one gets:

$$\sigma_e^{-+} > \sigma_e^{-0} > \sigma_e^{00} > \sigma_e^{--} > \sigma_e^{++} > \sigma_e^{+0} > \sigma_e^{+-}. \tag{14}$$

The case of a heavy right slepton may be realized in extended SUSY models ([11] and references therein).

Comparing (11) and (14) shows that polarizing both beams allows one to distinguish between a higgsino–like scenario and a gaugino–like scenario with dominating $\tilde{e}_L$ exchange. This is not possible if only the electron beam is polarized.

In Table 2 we show the cross sections for various polarization configurations for our scenarios A1, A2, and B at $\sqrt{s} = (m_{\tilde{\chi}^0_1} + m_{\tilde{\chi}^0_2}) + 30$ GeV for $P^3_- = 0, \pm 85\%$ and $P^3_+ = 0, \pm 60\%$. In the higgsino–like scenario B σ_e is approximately the same as in the gaugino–like scenarios A1 and A2, because $BR(\tilde{\chi}^0_2 \to \tilde{\chi}^0_1 e^+ e^-)$ is much smaller in scenario B than in A1 and A2.

For scenario B the sequence of the cross sections coincides with (11). One notices that one obtains the same ordering of the polarized cross sections for the gaugino–like scenario A1. This shows that the relative size of the cross sections sensitively depends on the mass difference between $\tilde{e}_L$ and $\tilde{e}_R$, which is rather small in scenario A1, $m_{\tilde{e}_L} - m_{\tilde{e}_R} = 44$ GeV. Comparing the sequence of cross sections for the gaugino–like scenario A2, see Table 2, with that for pure $\tilde{e}_R$ exchange, see (13), one sees a small influence of $\tilde{e}_L$ exchange despite the rather high $\tilde{e}_L$ mass, $m_{\tilde{e}_L} = 500$ GeV.

3.2 Lepton forward–backward asymmetry

Owing to the Majorana character of the neutralinos the angular distribution of the production process is symmetric under the exchange $\cos\Theta \leftrightarrow -\cos\Theta$, where Θ is the production angle of $\tilde{\chi}^0_j$ [12]. The angular distribution of the decay lepton ℓ^-, however, depends on the polarization of $\tilde{\chi}^0_j$. Since the longitudinal polarization Σ^3_P and the transverse polarization Σ^1_P of $\tilde{\chi}^0_j$ are forward–backward antisymmetric, the lepton forward–backward asymmetry A_{FB} of the decay lepton may become quite large. The lepton forward–backward asymmetry A_{FB} is defined as

$$A_{FB} = \frac{\sigma_e(\cos\Theta_e > 0) - \sigma_e(\cos\Theta_e < 0)}{\sigma_e(\cos\Theta_e > 0) + \sigma_e(\cos\Theta_e < 0)}, \tag{15}$$

where Θ_e is the angle between the electron beam and the outgoing ℓ^-. We will show A_{FB} not too far from threshold because it decreases with $\sqrt{s}$ for fixed neutralino masses.

In Figs. 3a–c we show A_{FB} of the decay electron as a function of the beam polarizations for the scenarios A1, A2, and B, respectively, at $\sqrt{s} = (m_{\tilde{\chi}^0_1} + m_{\tilde{\chi}^0_2}) + 30$ GeV. First one notices that by appropriately polarizing both beams one gets a larger asymmetry. Actually, in the scenarios A1 and B A_{FB} turns out to be practically zero for both beams unpolarized. The figures also exhibit a very different pattern. When comparing Fig. 3a with Fig. 3b, the different behaviour is due to the different masses of $\tilde{e}_L$. In the higgsino scenario B the asymmetries are much smaller. Notice again the symmetry of $P^3_- = \pm \leftrightarrow P^3_+ = \mp$ in scenario B as already observed in the total cross section. Measuring the lepton forward–backward asymmetry A_{FB} in addition to the total cross section strongly constrains the selectron masses $m_{\tilde{e}_L}$ and $m_{\tilde{e}_R}$ as well as the mixing properties of $\tilde{\chi}^0_1$ and $\tilde{\chi}^0_2$.

We also studied the dependence of the lepton forward–backward asymmetry A_{FB} on $\sqrt{s}$. For $\sqrt{s} \gg (m_{\tilde{\chi}^0_1} + m_{\tilde{\chi}^0_2})$ the angular distribution of the decay lepton is essentially the same as that of the decaying neutralino $\tilde{\chi}^0_2$ [13]. Therefore the lepton forward–backward asymmetry practically vanishes.

3.3 Opening angle distribution

The opening angle distribution between the two leptons from the decay $\tilde{\chi}^0_2 \to \ell^+\ell^-\tilde{\chi}^0_1$ is independent of spin correlations due to the Majorana nature of the neutralinos [14]. Therefore, it factorizes into a product of two expressions, one from production and the other from decay. For the same reason this is also valid for the energy distribution of the neutralino decay products. For both distributions it is suitable to parametrize the phase space by the scattering angle Θ between the incoming $e^-(p_1)$ beam and the outgoing neutralino $\tilde{\chi}^0_2(p_4)$, the azimuthal angle $\Phi_{\tilde{\chi}^0_2\ell^-}$ between the scattering plane and the $(\tilde{\chi}^0_2\ell^-)$–plane and the opening angle Θ_{+-} between the leptons ℓ^+ and ℓ^- from the decay of the neutralino $\tilde{\chi}^0_2$. The contributions of the transverse polarizations of the neutralino vanish after integration. As for the longitudinal polarization Σ^3_P, the Majorana character of the neutralino is crucial. If CP is conserved Σ^3_P is forward–backward antisymmetric, $\Sigma^3_P(-\cos\Theta) = -\Sigma^3_P(\cos\Theta)$, so that the contribution of the longitudinal polarization vanishes after integration over the scattering angle Θ [14].

In Figs. 4a and b we show the $\cos\Theta_{+-}$ distribution in the scenarios A1, A2 and B at $\sqrt{s} = (m_{\tilde{\chi}^0_1}+m_{\tilde{\chi}^0_2})+30$ GeV and for various beam polarizations. One notices that the shape of the Θ_{+-} distribution is mainly determined by the mixing character of the neutralinos. The selectron masses mainly influence the size of the cross section. Due to the factorization of production and decay the beam polarizations have no influence on the shape of this distribution.

3.4 Dependence on M_1

So far we have used the GUT relation (10) for the gaugino masses. In the following we will be more general and not use this relation [2, 13, 15, 16]. We will discuss the M_1 dependence of the cross section and the forward–backward asymmetry of the decay electron [7]. All other parameters are chosen as in scenario A1 except the mass of $\tilde{e}_R$, $m_{\tilde{e}_R} = 161$ GeV. The neutralino masses as well as the $Z^0\tilde{\chi}^0_i\tilde{\chi}^0_j$ couplings O''^L_{ij} and the $\tilde{\chi}^0_i\tilde{\ell}\ell$ couplings $f^{L,R}_{\ell i}$ depend on M_1.

In Fig. 5 we show the neutralino masses as function of M_1. The grey areas are excluded by the constraints $m_{\tilde{\chi}^0_1} < m_{\tilde{\chi}^\pm_1}$, $m_{\tilde{\chi}^0_1} > 35$ GeV. We see that $m_{\tilde{\chi}^0_1}$ depends very strongly on M_1 in the interval between -130 GeV$< M_1 < M_2$, whereas all other neutralino masses are nearly independent of M_1. On the other hand, in the region $M_2 \leq M_1 \leq |\mu|$ only $m_{\tilde{\chi}^0_2}$ depends strongly on M_1.

In the formulae for the cross section $\sigma(e^+e^- \to \tilde{\chi}^0_1\tilde{\chi}^0_2)$ and for the decay $\tilde{\chi}^0_2 \to \tilde{\chi}^0_1\ell^+\ell^-$ the products of couplings $f^L_{\ell 1}f^L_{\ell 2}$ and $f^R_{\ell 1}f^R_{\ell 2}$ enter. We therefore show for these products the dependence on M_1 in Fig. 6. We do not consider values $|M_1| > 160$ GeV, where $m_{\tilde{\chi}^0_2} > m_{\tilde{\ell}_R}$, because then the two–body decay $\tilde{\chi}^0_2 \to \tilde{\ell}_R + \ell$ would be the dominating decay channel. One observes a strong variation of $f^R_{\ell 1}f^R_{\ell 2}$ and $f^L_{\ell 1}f^L_{\ell 2}$ for $M_1 > 80$ GeV. In particular, $f^R_{\ell 1}f^R_{\ell 2}$ has a positive maximum at 140 GeV, whereas $f^L_{\ell 1}f^L_{\ell 2}$ is zero at $M_1 = 120$ GeV and reaches large negative values for $M_1 \geq 160$ GeV. We therefore have the following regions: $f^L_{\ell 1}f^L_{\ell 2} > f^R_{\ell 1}f^R_{\ell 2} > 0$ for -200 GeV$< M_1 < 80$ GeV, $|f^R_{\ell 1}f^R_{\ell 2}| > f^L_{\ell 1}f^L_{\ell 2}$ for 110 GeV$< M_1 < 140$ GeV, and $|f^L_{\ell 1}f^L_{\ell 2}| > f^R_{\ell 1}f^R_{\ell 2}$ for $M_1 > 150$ GeV. The coupling O''^L_{12} is small in this gaugino–like scenario.

Fig. 7a exhibits the M_1 dependence of $\sigma(e^+e^- \to \tilde{\chi}^0_1\tilde{\chi}^0_2) \times BR(\tilde{\chi}^0_2 \to e^+e^-\tilde{\chi}^0_1)$ at $\sqrt{s} = (m_{\tilde{\chi}^0_1} + m_{\tilde{\chi}^0_2}) + 30$ GeV in the region 40 GeV$<$ M_1 $<$160 GeV for various beam polarizations. Since the masses of $\tilde{e}_L$ and $\tilde{e}_R$ are in this case comparable, the curves reflect the behaviour of $f^L_{\ell 1}f^L_{\ell 2}$ and $f^R_{\ell 1}f^R_{\ell 2}$ of Fig. 6. A left (right) beam polarization of the electron (positron) selects the $\tilde{e}_L$ exchange, while the maximum in the curve with a right (left) electron (positron) polarization is due the maximum of $f^R_{\ell 1}f^R_{\ell 2}$ in Fig. 6.

Fig. 7b shows the analogous curves for a heavy $\tilde{e}_L$ with $m_{\tilde{e}_L} = 500$ GeV. One clearly sees that the $\tilde{e}_L$ exchange is strongly suppressed, and one obtains higher cross sections for right polarized e^- beams.

We have also studied the M_1 dependence of the forward–backward asymmetry A_{FB} of the decay electron, eq. (15), shown in Fig. 8 for $m_{\tilde{e}_L} =$ 176 GeV and $m_{\tilde{e}_L} = 500$ GeV. One notices a significant variation with M_1 and a strong dependence on the beam polarizations. Comparing Fig. 8a and b, one observes a pronounced difference of the forward–backward asymmetry of the decay electron in the region 40 GeV$< M_1 <$100 GeV. This is due to the suppression of $\tilde{e}_L$ exchange in Fig. 8b. The beam polarizations enhance the effect considerably. The behaviour at $M_1 \approx 120$ GeV is again due to the maximum of $f^R_{\ell 1}f^R_{\ell 2}$.

4 Conclusions

The objective of this paper has been twofold. Firstly, we have studied the advantage of having both the e^- and the e^+ beam polarized. If the polarizations of e^- and e^+ are varied, the relative size of the cross sections depends significantly on the mixing character of the neutralinos and on the masses of

$\tilde{e}_L$ and $\tilde{e}_R$. By an appropriate choice of polarizations one can obtain up to three times larger cross sections than in the unpolarized case. Secondly, by taking into account the full spin correlations between production and decay, we have studied the angular distribution, as well as the forward–backward asymmetry of the decay electron $e^+e^- \to \tilde{\chi}^0_1\tilde{\chi}^0_2$, $\tilde{\chi}^0_2 \to \tilde{\chi}^0_1 e^+e^-$. Measuring this asymmetry for various beam polarizations strongly constrains the masses of $\tilde{e}_L$ and $\tilde{e}_R$ and the mixing properties of the neutralinos. We have also studied the dependence on the gaugino mass parameter M_1. For a determination of M_1 the use of polarized e^+ and e^- beams would be very helpful. Due to the Majorana character of the neutralinos the opening angle distribution between the decay leptons is independent of spin correlations. It is very sensitive to the mixing character of the neutralinos, whereas its shape is only weakly dependent on the selectron masses.

Acknowledgments

We thank U. Martyn for many valuable discussions. We are grateful to W. Porod and S. Hesselbach for providing the computer programs for neutralino widths. G.M.-P. was supported by *Friedrich-Ebert-Stiftung*. This work was also supported by the German Federal Ministry for Research and Technology (BMBF) under contract number 05 7WZ91P (0), by the Deutsche Forschungsgemeinschaft under contract Fr 1064/4-1, and the 'Fonds zur Förderung der wissenschaftlichen Forschung' of Austria, Project No. P13139-PHY.

References

[1] G. Moortgat–Pick, S. Hesselbach, F. Franke, H. Fraas, hep-ph/9909549, to be published in the Proceedings of 4th International Workshop on Linear Colliders (LCWS 99), Sitges, Barcelona, Spain, 28 April - 5 May 1999; S. Hesselbach, F. Franke, H. Fraas, WUE-ITP-2000-008, to appear in the Proceedings of the 2nd Joint ECFA/DESY study on Physics and Detectors for a Linear Electron-Positron Collider.

[2] S.Y. Choi, A. Djouadi, H. Dreiner, J. Kalinowski, P. Zerwas, Eur. Phys. J. **C 7** (1999) 123; S.Y. Choi, A. Djouadi, H.S. Song, P. Zerwas, Eur. Phys. J. **C 8** (1999) 669; S.Y. Choi, M. Guchait, J.Kalinowski, P.M. Zerwas, hep-ph/0001175; S.Y. Choi, A. Djouadi, M. Guchait, J. Kalinowski, H.S. Song, P.M. Zerwas, hep-ph/0002033.

[3] G. Moortgat–Pick, H. Fraas, A. Bartl, W. Majerotto, Eur. Phys. J. **C 7** (1999) 113; G. Moortgat–Pick, H. Fraas, Acta Phys. Polon. **B 30**

(1999) 1999.

[4] A. Bartl, H. Fraas, W. Majerotto, Nucl. Phys. **B 278** (1986) 1; A. Bartl, H. Fraas, W. Majerotto, N. Oshimo, Phys. Rev. **D 40** (1989) 1594; A. Bartl, W. Majerotto, B. Mösslacher, in 'e^+e^- Collisions at 500 GeV: The Physics Potential', Part B, DESY 92–123B, p. 641, ed. by P.M. Zerwas.

[5] S. Ambrosanio, B. Mele, Phys. Rev. **D 52** (1995) 3900; S. Ambrosanio, B. Mele, Phys. Rev. **D 53** (1996) 2541.

[6] G. Moortgat–Pick, H. Fraas, Phys. Rev. **D 59** (1999) 015016.

[7] G. Moortgat–Pick, H. Fraas, A. Bartl, W. Majerotto, Eur. Phys. J. **C9** (1999) 521; Eur. Phys. J. **C9** (1999) 549 (E).

[8] H.E. Haber, G.L. Kane, Phys. Rep. **117** (1985) 75.

[9] S. Ambrosanio, G.A. Blair, P. Zerwas, ECFA-DESY LC-Workshop, 1998, http://www.desy.de/conferences/ecfa-desy-lc98.html.

[10] G. Moortgat–Pick, PhD Thesis, Würzburg 1999, ISBN 3-8265-6981-4.

[11] S. Hesselbach, PhD Thesis, Würzburg 1999.

[12] S.M. Bilenky, E.C. Christova, N.P. Nedelcheva, Bulg. Jour. of Phys. **13** (1986) 283.

[13] J.L. Feng, M.J. Strassler, Phys. Rev. **D 55** (1997) 1326.

[14] G. Moortgat–Pick, H. Fraas, in preparation.

[15] SLAC–Report 485, submitted to *Snowmass 1996.*

[16] J.L. Kneur, G. Moultaka, Phys. Rev. **D 59** (1999) 015005.

	M_2	μ	$m_{\tilde{e}_L}$	$m_{\tilde{e}_R}$	$m_{\tilde{\chi}^0_1}$	$m_{\tilde{\chi}^0_2}$	$\Gamma_{\tilde{\chi}^0_2}$	O''^L_{12}	$f^L_{\ell 1} f^L_{\ell 2}$	$f^R_{\ell 1} f^R_{\ell 2}$
A1	152	316	176	132	71	130	25E−6	−.02	−.20	−.12
A2	152	316	500	132	71	130	15E−6	−.02	−.20	−.12
B	250	125	176	132	71	130	369E−6	+.39	2E−5	.027

Table 1: Parameters, masses, and total $\tilde{\chi}^0_2$ width (in GeV) and couplings in scenarios A1, A2, and B for $\tan\beta = 3$.

	$\sqrt{s} = (m_{\tilde{\chi}^0_1} + m_{\tilde{\chi}^0_2}) + 30$ GeV						
A1	$(-+)$	$(+-)$	(-0)	(00)	$(+0)$	$(--)$	$(++)$
σ_e/fb	10.2	6.7	6.6	5.6	4.6	3.1	2.5
A2	$(+-)$	$(+0)$	(00)	$(++)$	$(-+)$	(-0)	$(--)$
σ_e/fb	9.5	6.0	3.6	2.5	1.3	1.1	1.0
B	$(-+)$	$(+-)$	(-0)	(00)	$(+0)$	$(--)$	$(++)$
σ_e/fb	21.7	19.0	14.3	13.5	12.7	6.8	6.4

Table 2: Polarized cross sections $\sigma_e = \sigma(e^+e^- \to \tilde{\chi}^0_1\tilde{\chi}^0_2) \times BR(\tilde{\chi}^0_2 \to \tilde{\chi}^0_1 e^+e^-)$/fb at $\sqrt{s} = m_{\tilde{\chi}^0_2} + m_{\tilde{\chi}^0_1} + 30$ GeV in scenarios A1, A2, and B, see Table 1, for unpolarized beams (00), only electron beam polarized (-0), $(+0)$ with $P^3_1 = \pm 85\%$ and both beams polarized with $P^3_1 = -85\%$, $P^3_2 = +60\%$ $(-+)$ and $P^3_1 = +85\%$, $P^3_2 = -60\%$ $(+-)$.

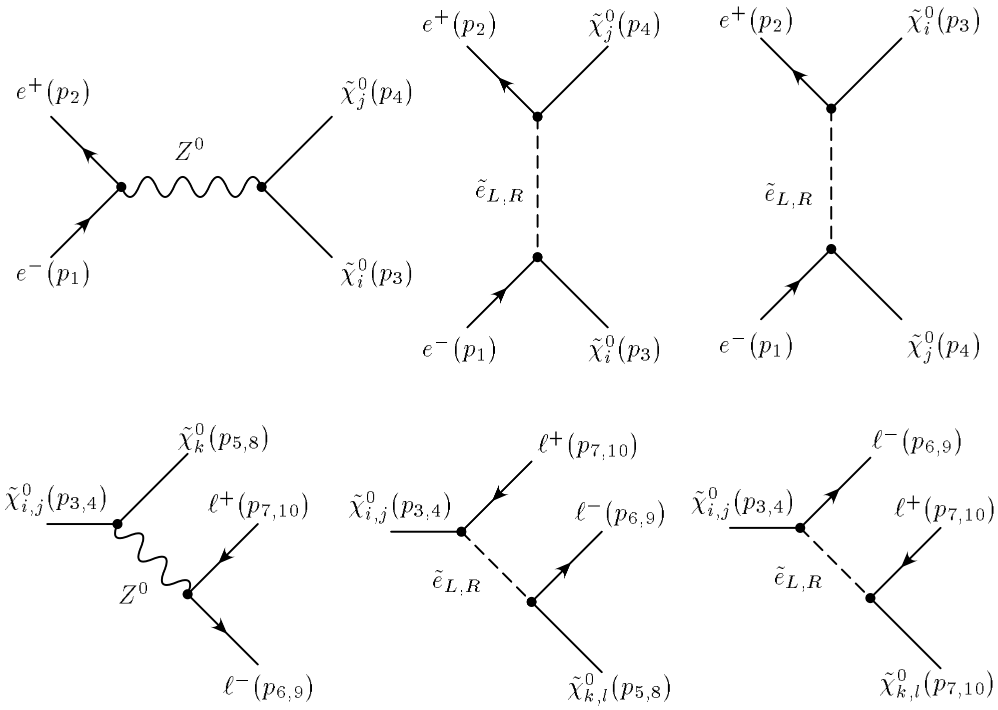

Figure 1: Feynman diagrams for neutralino production $e^-(p_1)e^+(p_2) \to \tilde{\chi}^0_i(p_3)\tilde{\chi}^0_j(p_4)$ and the decay processes $\tilde{\chi}^0_i(p_3) \to \tilde{\chi}^0_k(p_5)\ell^+(p_6)\ell^-(p_7)$ and $\tilde{\chi}^0_j(p_4) \to \tilde{\chi}^0_l(p_8)\ell^+(p_9)\ell^-(p_{10})$.

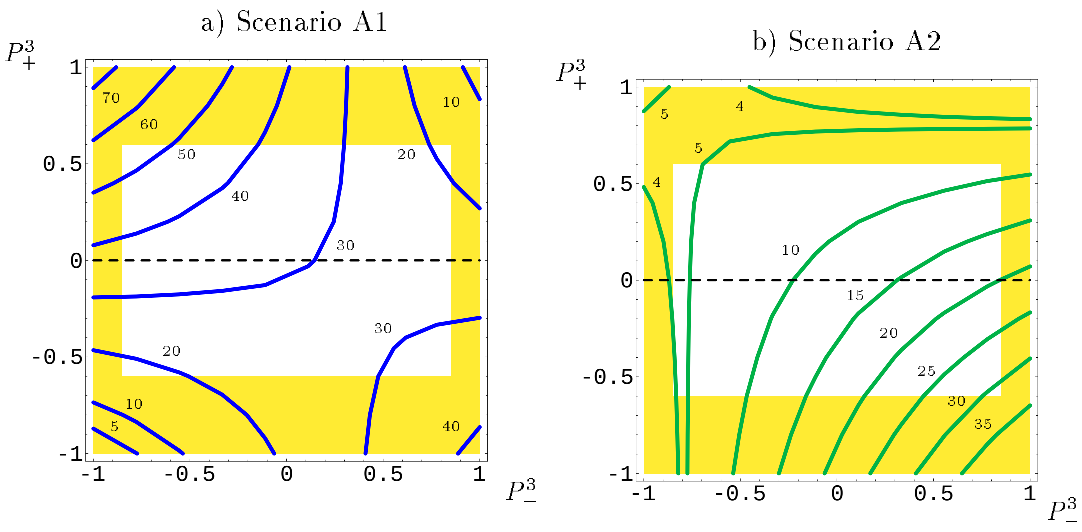

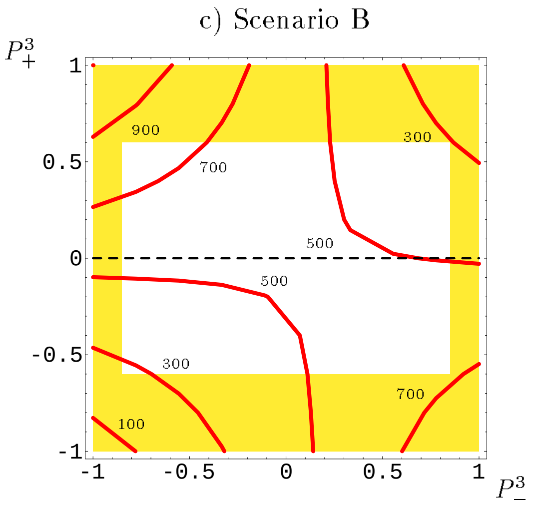

Figure 2: Contour lines of cross sections $\sigma(e^+e^- \to \tilde{\chi}_1^0\tilde{\chi}_2^0)$ in fb at $\sqrt{s} = (m_{\tilde{\chi}_1^0} + m_{\tilde{\chi}_2^0}) + 30$ GeV in the gaugino–like scenarios a) A1, b) A2 and in c) the higgsino–like scenario B (see Table 1). The longitudinal beam polarization for electrons (positrons) is denoted by P_-^3 (P_+^3). The white region is accessible for $|P_-^3| < 85\%$, $|P_+^3| < 60\%$ (dashed–line if only electron beam polarized).

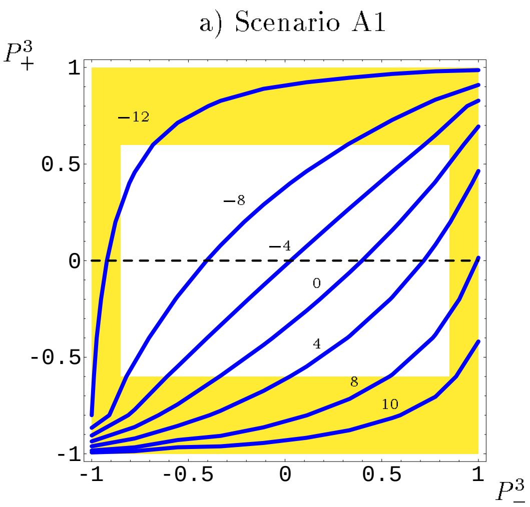

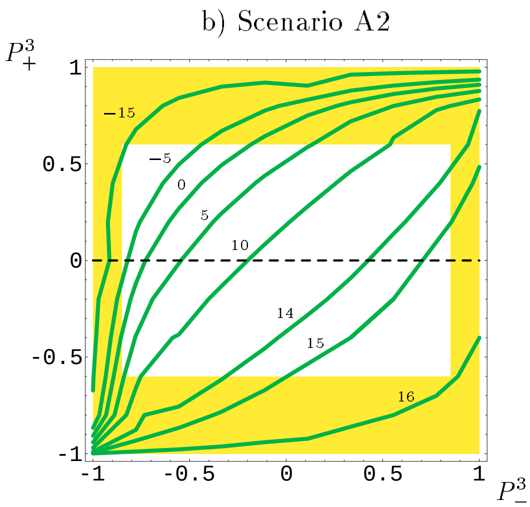

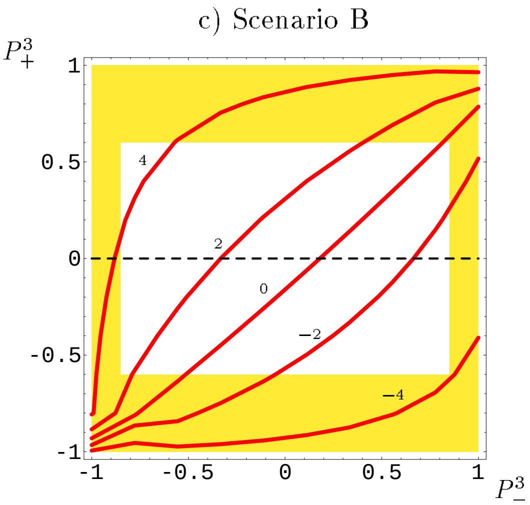

Figure 3: Contour lines of the forward–backward asymmetry of the decay electron $A_{FB}/\%$ of $e^+e^- \to \tilde{\chi}_1^0\tilde{\chi}_2^0, \tilde{\chi}_2^0 \to \tilde{\chi}_1^0 e^+e^-$ at $\sqrt{s} = (m_{\tilde{\chi}_1^0} + m_{\tilde{\chi}_2^0}) + 30$ GeV in the gaugino-like scenarios a) A1, b) A2, and in c) the higgsino–like scenario B (see Table 1). The longitudinal beam polarization for electrons (positrons) is denoted by P_-^3 (P_+^3). The white region is accessible for $|P_-^3| < 85\%$, $|P_+^3| < 60\%$ (dashed–line if only electron beam polarized).

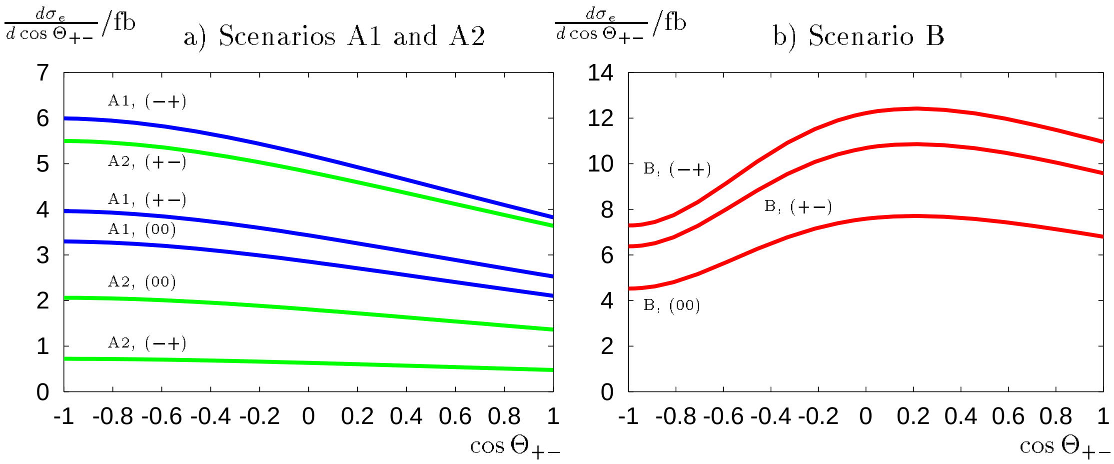

Figure 4: Opening angle distribution of the decay leptons from $e^+e^- \to \tilde{\chi}_1^0\tilde{\chi}_2^0$, $\tilde{\chi}_2^0 \to e^+e^-\tilde{\chi}_1^0$ in the gaugino–like scenarios a) A1, A2 and in b) the higgsino–like scenario B (see Table 1) at $\sqrt{s} = (m_{\tilde{\chi}_1^0} + m_{\tilde{\chi}_2^0}) + 30$ GeV for unpolarized beams (00), for $P_- = -85\%$, $P_+ = +60\%$ $(-+)$ and for $P_- = +85\%$, $P_+ = -60\%$ $(+-)$, respectively.

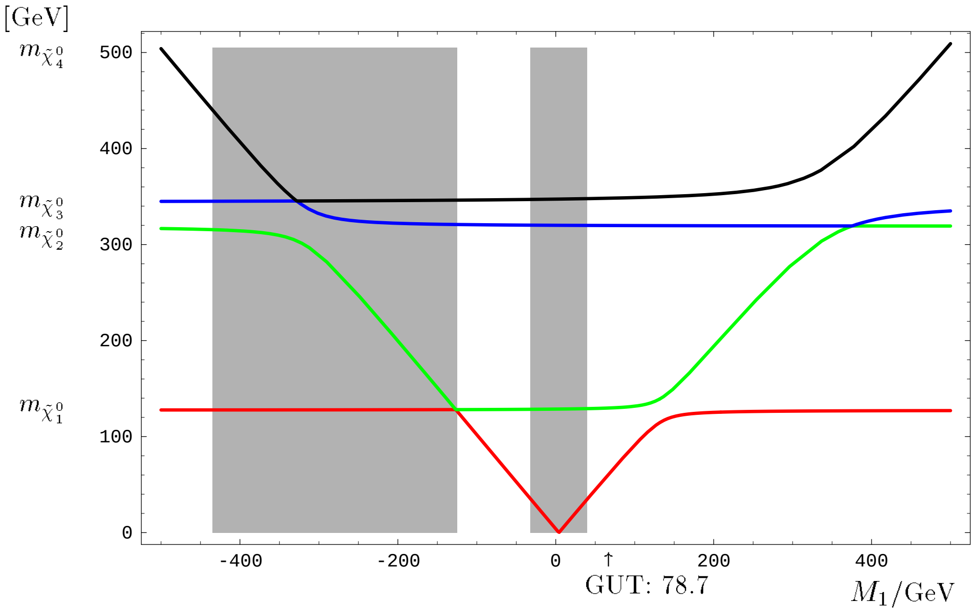

Figure 5: Neutralino mass spectrum as a function of M_1 in the range -500 GeV$< M_1 < 500$ GeV. The grey areas are excluded by the constraints $m_{\tilde{\chi}_1^0} < m_{\tilde{\chi}_1^\pm}$, $m_{\tilde{\chi}_1^0} > 35$ GeV. All other MSSM parameters as in scenario A1; GUT relation (10) gives $M_1 = 78.7$ GeV.

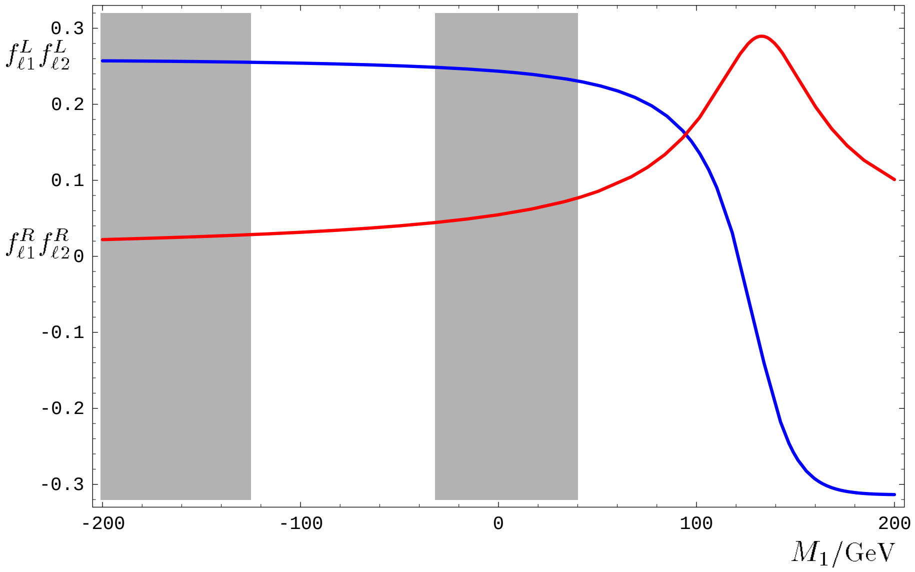

Figure 6: Slepton couplings $f^L_{\ell 1} f^L_{\ell 2}$ and $f^R_{\ell 1} f^R_{\ell 2}$ as a function of M_1 in the range -200 GeV$< M_1 < 200$ GeV. All other MSSM parameters as in scenario A1; GUT relation (10) gives $M_1 = 78.7$ GeV.

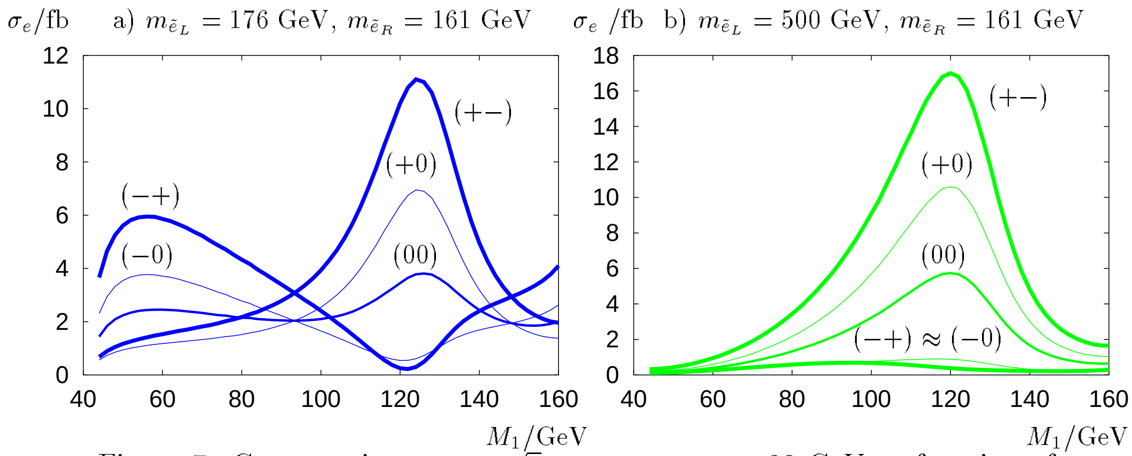

Figure 7: Cross sections σ_e at $\sqrt{s} = m_{\tilde{\chi}^0_1} + m_{\tilde{\chi}^0_2} + 30$ GeV as function of gaugino parameter M_1 for unpolarized beams (00), for only electron beam polarized (−0), (+0) with $P^3_- = \pm 85\%$ and for both beams polarized (−+), (+−) with $P_- = \mp 85\%$, $P_+ = \pm 60\%$. The slepton masses are a) $m_{\tilde{e}_L} = 176$ GeV, $m_{\tilde{e}_R} = 161$ GeV, and b) $m_{\tilde{e}_L} = 500$ GeV, $m_{\tilde{e}_R} = 161$ GeV; the other SUSY parameters as in scenario A1.

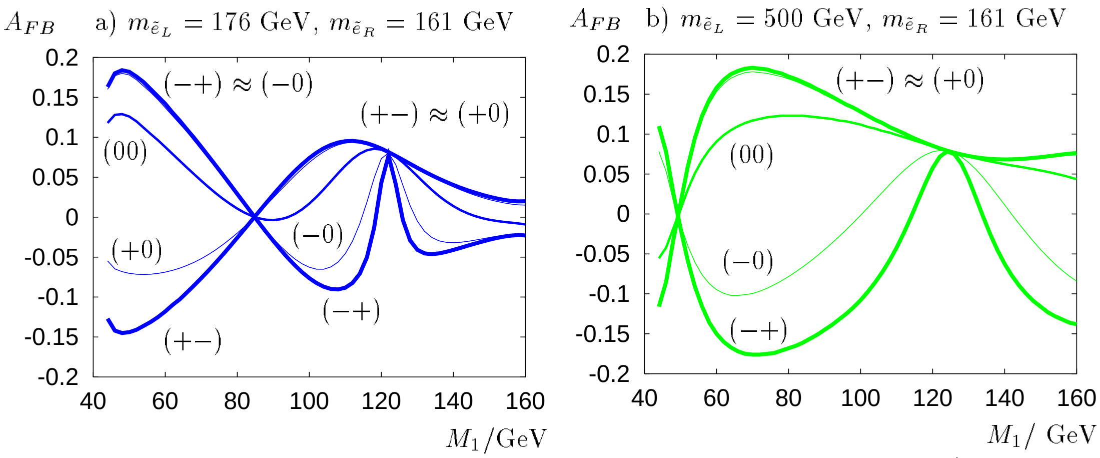

Figure 8: Forward–backward asymmetry of decay electron A_{FB} of $e^+e^- \to \tilde{\chi}^0_1\tilde{\chi}^0_2$, $\tilde{\chi}^0_2 \to \tilde{\chi}^0_1 e^+ e^-$ at $\sqrt{s} = m_{\tilde{\chi}^0_1} + m_{\tilde{\chi}^0_2} + 30$ GeV as function of gaugino parameter M_1 for unpolarized beams (00), for only electron beam polarized (-0), $(+0)$ with $P^3_- = \pm 85\%$ and for both beams polarized $(-+)$, $(+-)$ with $P_- = \mp 85\%$, $P_+ = \pm 60\%$. Slepton masses are a) $m_{\tilde{e}_L} = 176$ GeV, $m_{\tilde{e}_R} = 161$ GeV, and b) $m_{\tilde{e}_L} = 500$ GeV, $m_{\tilde{e}_R} = 161$ GeV; the other SUSY parameters as in scenario A1.